

Theory and experiments on periodic lattice distortions that explain 1D conductivity along the CuO₂ plane ab and a-b diagonals in YBa₂Cu₃O₇ (YBCO) 50 nm film with a 24 DEG grain boundary (GB)

H.S. Sahibudeen, M.A. Navacerrada and J.V. Acrivos

San José State University, San José CA95192-0101 TEL: 408 924 4987/4972, FAX 408 924 4945

Email: hizamss@yahoo.com; m_navacerrada@hotmail.com; jacrivos@athens.sjsu.edu

ABSTRACT

Self consistent field (SCF) calculations carried out using MOLECOLE Linux codes for a lamella L in the nano-particle [T²-Nd₂CuO₄]₁₈ explain the d_{xy} symmetry of the periodic lattice distortions (PLD) observed in X-ray diffraction (XRD) along preferred superconductivity direction, ab and a-b diagonals in the material CuO₂ plane.

Keywords: cuprate superconductor, XRD, XAS, SCF

INTRODUCTION

The continuous overlap along the O:2p_{xy} sigma orbital in the highest/lowest occupied molecular orbital (HOMO/LUMO) for the CuO₂ plane of cuprate superconductors showed that continuous 1D electron density, ρ_e appeared only along the ab (a-b) diagonals [1], in agreement with the preferred direction of superconductivity found later [2]. The continuous ρ_e in the material also governs the direction of 1D charge density waves (CDW) causing the PLD, observed in X-ray diffraction (XRD) [2]. This work describes the effects of a PLD by SCF calculations.

EXPERIMENTAL

XRD and X-ray absorption spectra (XAS) in fluorescence (F) were measured at the Stanford Synchrotron Radiation Laboratory (SSRL) and at the Lawrence Berkeley National Laboratory (LBNL-station 6.3.1 of the ALS) on 50 nm c-axis oriented YBCO films deposited on single crystal SrTiO₃ and bi-crystals with a 24° grain boundary (GB) at the Complutense University [4] (FIG. 1, 2).

DISCUSSION

The (HKL) = (1±12),(114),(221),(2±22),(224) planes (FIG. 1) intersect the PLD, **q** = (q_xq_yq_z) to produce XRD sidebands of intensity A_{±1} relative to the center band A₀, independent of L and E = 8048 to 7040 eV (FIG. 1). Rocking curves plotted versus sa²ds/H (s = 2E sin(θ)/hc = scattering vector, h = Planck constant, c = velocity of light, θ = Bragg angle,

χ,φ constant, and dH/H = dK/K = dL/L) obtain 2q_x = 2dH_{XRD,SB} ~ 1/12 [2]. H, K scans with dL=0 give sidebands at -dH_{XRD,SB} = dK_{XRD,SB} =>q_x = -q_y when K=H>> L≠0, which identify **q** as a transverse wave along the ab diagonal in the CuO₂ plane. Thus the distortion at site **R** is caused by the transverse wave **u** exp(i(2π**R**·**q**+φ)), **u/a** = (u_x -u_xq_x/q_y 0) when a is the unit axis. The relative sideband intensities [2]:

A₀/A_{±1} = |J₀(z_{H±HL})/J_{±1}(z_{H±HL})|², z_{H±HL} = 4πu_xH where the J_n, Bessel functions of the first order obtain u_x = 0.1 ± 0.01. The effect of the PLD is simply to produce a twist of the 4 O relative to the center Cu atom (FIG. 3).

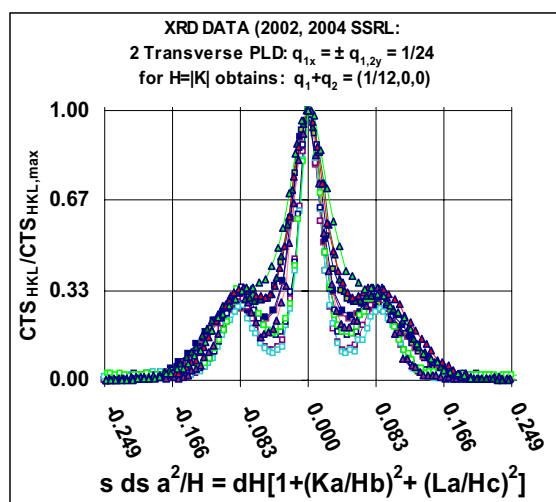


FIG. 1: Film rocking curves for (H K=±H L≠0).

The main effect of the PLD is to focus the transport in 1D. A unique uniform 1D electron density along the ab, a-b diagonals of the CuO₂ plane for the Cu₄O₄ lamella HOMO/LUMO (FIG. 4) coincides with the directions of preferred superconductivity [3], normal to the 1D distortion CDW. The PLD are evident in XRD only when planes along the diagonal in reciprocal space (K = ± H) intersect **q** (FIG. 1).

SCF calculations can determine how the total energy and especially how the Mulliken overlap population (M-OP) ∝ ρ_e along a given bond depend on **q** as the CDW moves in the lattice.

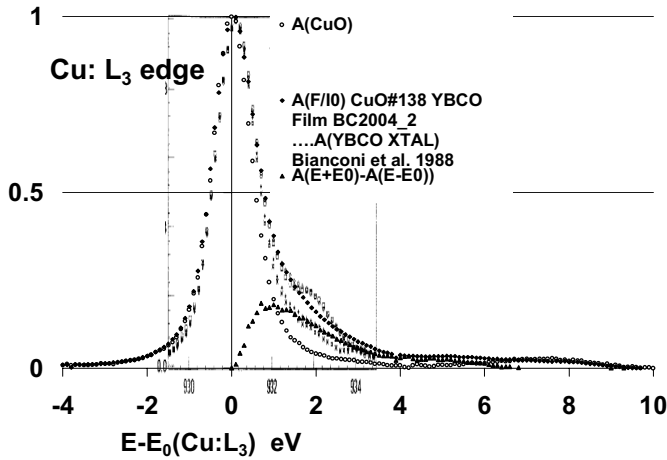


FIG. 2: Cu L₃ edge Absorbance, A for $\text{YBa}_2\text{Cu}_3\text{O}_{7-\delta}$ film compared to CuO reference and single crystal with different oxygen content, π : $\delta=0$, o.x. : $\delta > 0.15$ [ref. 5].

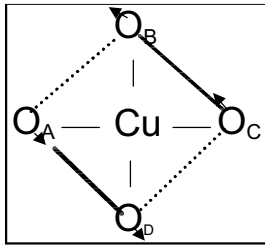


FIG. 3: Relative O atom motion with respect to Cu produced by transverse wave PLD.

The OP depends on the bond distance, but in the presence of a PLD, only $O_A-O_D=O_B-O_C=a/2^{1/2}$ remains constant (FIG. 3). All the other bond distances vary with sinusoidal amplitude less than $u_x \sin(2\pi q_x/2) \sim 0.013$. This means that 1D electron conductivity due to MO overlap is favored along the direction of constant bond distance in the presence of a PLD. Since the HOMO are doubly degenerate, with $O:2p_{xy}-O:2p_{xy}$ overlap preferred along either ab and/or $a-b$ diagonals (FIG. 4), two PLD normal to the diagonals are present in separate domains, and/or twin crystals. The 1D uniform ρ_e for N atom, n_a, n_b chains (FIG. 4) are described by Tight Binding, Alternant, LCAO-MO:

$$\begin{aligned} \chi_{O, \text{chain } n_a, n_b}(\mathbf{r}, \pi, \pi, k_z) &= (2N)^{-1/2} i \cos(\pi(n_a + n_b)) \sum_{\text{chain O}} [\psi_O(\mathbf{r}-\mathbf{R}_{O3a}) - \psi_O(\mathbf{r}-\mathbf{R}_{O3b})], \\ \chi_{Cu, n_a, n_b}(\mathbf{r}, \pi, \pi, 0) &= N^{-1/2} \cos(\pi(n_a + n_b)) \sum_{\text{chain Cu}} \psi_{Cu}(\mathbf{r}-\mathbf{R}_{Cu}), \\ \chi_{\text{donor D } n_a, n_b}(\mathbf{r}, \pi, \pi, k_z) &= N^{-1/2} \cos(\pi(n_a + n_b)) \sum_{\text{chain D}} \psi_D(\mathbf{r}-\mathbf{R}_D). \end{aligned}$$

$\psi_M = M$ atomic orbital at \mathbf{R} , $k_x = k_y = \pi$, $k_z = 0$.

The predictive power of a continuous electron density in real space HOMO, shows the cause of PLD: oscillations in localized energy and charge at individual lamellae that is compensated in the 24 by 24 cell, and

by a variation in the Mulliken overlap population of one percent in other directions is sufficient to focus 1D conductivity along a unique diagonal (FIG. 5a-d). Only a unique constant bond distance, e.g., $O_A-O_D = O_B-O_C$ (FIG. 3) can give a constant overlap population: $OP(O_A-O_D) = OP(O_B-O_C) = -0.79$ that gives rise to continuous overlap conductivity.

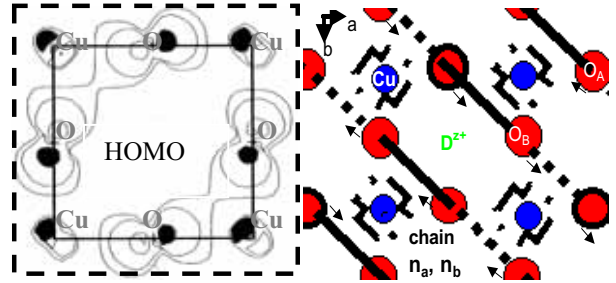


FIG. 4: HOMO electron density in CuO_2 plane, $\rho_e > 10^{-3} \text{ bohr}^{-3}$ along ab and $a-b$ diagonals [ref. 1] indicate the shape of the ball and stick model near the Fermi level: $MO < 0$; ... $MO > 0$; -.

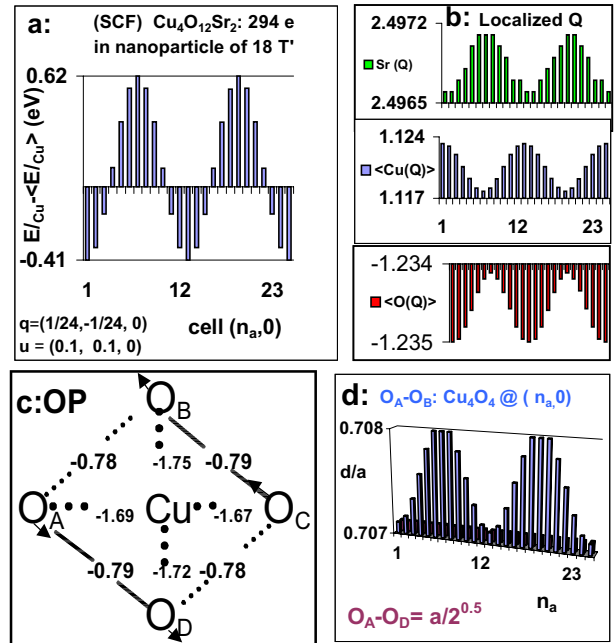


FIG. 5: SCF calculations as PLD wave moves through origin of $\text{Cu}_4\text{O}_{12}\text{Sr}_2[\text{T}'\text{Nd}_2\text{CuO}_4]_{18}$: **a:** Total electronic energy deviation from $\langle E \rangle$ per Cu atom **b:** Localized charge Q at atoms in each of 24 lamella. **c:** Mulliken OP $\propto \rho_e$ in given bonds. **d:** O_A-O_B bond distance along a -axis [ref. 2].

Charge transfer to lamella $L^{+z} = \text{Cu}_4\text{O}_{12}\text{Sr}_2^{+z}$ within $[\text{T}'\text{-Nd}_2\text{CuO}_4]_{18}$ contributes to the transport properties of the material. The ab-initio SCF calculation shows how the stability $E_{\text{total}} - E_{\text{atoms}}$ and

charge, $Q(M)$ at atom M in L changes and as the CDW passes through the center (Table I): $Q(O)$ remains almost constant with charge transfer of $\pm 2 e$ to 14 unit cells, indicating that the $O:2p_{xy}-O:2p_{xy}$ form covalent bonds. $Q(Cu)$ varies slightly more but the Sr atom ionizes according to the amount of charge transfer, indicating that the ionic layers act as a buffer. A neutral lamella L^0 and the positively charged L^{+2} obtain a SCF ground state with $Q(Sr) = 2.5$. Donors that produce L^{-2} obtain $Q(Sr) = 0.6$ in the SCF ground state, indicating that the optimum number of electrons in the CuO_2 covalent layer is controlled by the alkaline earth atom which can take on multiple valence. The positively charged L^{+2} is most unstable, with the largest CDW variation. The optimum SCF ground state charge $Q(Cu)$ and $Q(O)$ indicate that the total electronic charge is not localized as in an ionic lattice but distributed in the covalent bonds.

L in [T ⁺ -Nd ₂ CuO ₄] ₁₈	E-E _a eV	<Q(Sr)>	<Q(Cu)>	<Q(O)>
L ⁻²	-38.7	0.6	1.3	-1.2
L ⁻² CDW % DEV	0.3	0.1	0.3	0.1
L ⁺⁰	-38.7	2.5	1.1	-1.3
L ⁺⁰ CDW % DEV	0.3	0.01	0.3	0.1
L ⁺²	-37.4	2.5	1.6	-1.3
L ⁺² CDW % DEV	0.3	1	0.5	0.1

Table I: SCF ground state energy stability, $E - E_a = (E_{total} - E_{atoms})/18$, average charges $\langle Q(M) \rangle$ at atoms, M in L^{+z} and percent deviation produced by CDW for different amount of charge transfer $\pm z$.

The YBCO film $Cu L_3$ edge white line absorbance, $A = F/I_0$ ($c \wedge \epsilon_{X-rays} = \pi/4$) shows a Gaussian shape for $E < E_0$, the edge threshold where it is comparable to A for CuO and YBCO single crystal and powders with a maximum oxygen content [5]. Many electron interactions in bulk metals may be responsible for enhanced absorption due to interactions near the Fermi energy when $E > E_0$ [6] but there is evidence for an X-ray exciton peak, 0.6 eV above E_0 when the absorption for the Gaussian shaped reference, $A(CuO)$ is subtracted from $A(F/I_0 \text{ YBCO film})$ (FIG. 2) [7 - 9]. The fully oxygenated samples [5] also show deviation from a Gaussian shape, 0.6 eV above E_0 , but, the peak associated by Bianconi et al. with superconductivity in fully oxygenated YBCO powders and single crystals is 2 eV above E_0 and appears to be also present in the film though weaker than the exciton peak. Both CuO and YBCO film show an absorption peak 7 eV above E_0

which can not be due to interactions near the Fermi level because CuO is not a metal.

A valid question is how does a PLD favor two electron Bose pairing for superconductivity? A possible answer is that a change in direction from an ab to $a-b$ chain needs to break an $O:2p_{xy}$ bond (FIG. 6), producing free electrons that interact with cation chain states, Cu or $D = Ba, Y$ (FIG. 4).

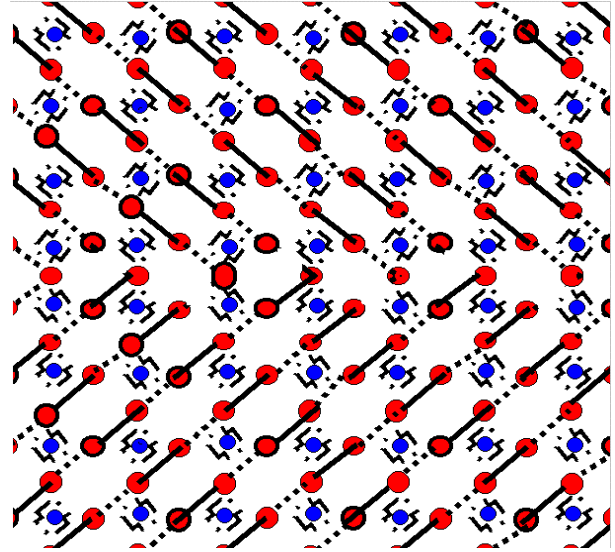


FIG. 6: Ball and stick model of PLD formation by breaking $O:2p_{xy}$ bonds along a chain. A 24 by 24 PLD arises when one bond in a 24 atom chain is broken, at an energy cost of one 24th of the neighbor resonant $O:2p_{xy}-O:2p_{xy}$ integral [ref. 9].

An electron pair obeying Bose statistics may be formed by the coupling of angular momenta in different chains, say an $O:2p_{3/2}$ chain defect electron with another in say, a $Cu:3d_{3/2}$ and/or $Ba:5d_{3/2}$ chain (FIG. 6) such that the sum $J = J_1 + J_2 = J_z = 0$. Eigenfunctions of J and J_z but not S_z of even parity for exchange, P_{12} of electrons 1 and 2 in $e_1 e_2^-$ obtain product states arising from $d_{3/2}(Cu \text{ or } Ba)$ and $p_{3/2}(O)$ chains: $|J, 0\rangle$, $J = 3, 1, 0$ with parity $P = 2\pi$:

$$\begin{array}{l}
 |J, J_z\rangle \quad P = \\
 \begin{array}{l}
 |3, 0\rangle \quad 2\pi \\
 |2, 0\rangle \quad \pi \\
 |1, 0\rangle \quad 2\pi \\
 |0, 0\rangle \quad 2\pi
 \end{array}
 \end{array}
 =
 \begin{array}{l}
 \text{Matrix} \\
 \begin{array}{l}
 40^{-1/2} \begin{bmatrix} 3 & 3 & 1 & 1 \end{bmatrix} \\
 8^{-1/2} \begin{bmatrix} -1 & -1 & 1 & 1 \end{bmatrix} \\
 40^{-1/2} \begin{bmatrix} 1 & 1 & -3 & -3 \end{bmatrix} \\
 8^{-1/2} \begin{bmatrix} 1 & -1 & 1 & -1 \end{bmatrix}
 \end{array}
 \end{array}
 *
 \begin{array}{l}
 \text{Coefficients} \\
 \begin{array}{l}
 (I+e^{iP} P_{12}) |3/2 \ 1/2\rangle_{d_1} * |3/2 \ -1/2\rangle_{p_2} \\
 (I+e^{iP} P_{12}) |3/2 \ -1/2\rangle_{d_1} * |3/2 \ 1/2\rangle_{p_2} \\
 (I+e^{iP} P_{12}) |3/2 \ 3/2\rangle_{d_1} * |3/2 \ -3/2\rangle_{p_2} \\
 (I+e^{iP} P_{12}) |3/2 \ -3/2\rangle_{d_1} * |3/2 \ 3/2\rangle_{p_2}
 \end{array}
 \end{array}
 \end{array}$$

where the matrix coefficients are obtained to satisfy the eigenvalues of $J^2 = J(J+1)$, J_z , and the

raising and lowering angular momentum textbook operations [10]. \mathbf{I} is the identity operator and electrons 1 and 2 are identified by the position in the product. When the principal axis of quantization is chosen parallel to a diagonal, $\mathbf{k} = \pm(\pi \pm\pi \ 0)$, the $e_1 e_2^-$ product state $|0,0\rangle$ of even exchange parity is written:

$$|0,0\rangle_{\text{chain jj coupling}} = 5^{-1/2} [\mathbf{I} + \mathbf{P}_{12}] / N$$

$$\left\{ \sum_M Y_{1,0\uparrow} [R_{O:2p}(\mathbf{r}-\mathbf{R}_{O3a}) - R_{O:2p}(\mathbf{r}-\mathbf{R}_{O3b})]_1 \right.$$

$$* \sum_M [Y_{2,0\downarrow} R_{Cu:3d}(\mathbf{r}-\mathbf{R}_{Cu})]_2$$

$$- \sum_M Y_{1,0\downarrow} [R_{O:2p}(\mathbf{r}-\mathbf{R}_{O3a}) - R_{O:2p}(\mathbf{r}-\mathbf{R}_{O3b})]_1$$

$$\left. * \sum_M [Y_{2,0\uparrow} R_{Cu:3d}(\mathbf{r}-\mathbf{R}_{Cu})]_2 \right\}.$$

where $Y_{l,m}(\theta_M, \phi_M)$ are spherical harmonics, the sub indexes $\uparrow\downarrow$ represent the spin $s_z = \pm 1/2$ states and $R_{n,l}(r_M)$ is the atomic orbital radial dependence when (r_M, θ_M, ϕ_M) are the spherical polar coordinates of an electron relative to atom $M = 1$ to N in chain.

The elegant work of S.C. Zhang et al. [11] helps to unravel the YBCO₇ superconductivity-magnetism relation. They have shown that spin polarized transport is non-dissipating and that transport by a Bose condensate in the superconducting state is a sub-group of spin polarized transport. Many questions remain but a really important one is to distinguish whether spin polarized Cu:3d_{3/2} states populated over the 3d_{5/2} band states interact with O:2p_{3/2} chain defects to obtain Bose condensation in superconducting YBCO₇ and/or can an uneven spin population in 1D conjugate orbitals involving the O:2p_{3/2} chains interacting with Ba and Y nd_{3/2} and 4f_{3/2} chains achieve Bose condensation?

CONCLUSION

The experimental study of PLD was inspired by SCF calculations which first indicated the unique direction of continuous 1 D electron density along O:2p sigma orbitals parallel to the CuO₂ plane diagonals in superconducting cuprates. The formation of Bose pairs between free electrons in PLD related oxygen chain defects with cation chains in YBCO is not limited to the CuO₂ plane. Ba/Sr/Y/La atoms can form J₁, J₂ coupled chains as long as even parity product states $J = J_1 + J_2 = 0 = J_z$ are formed.

ACKNOWLEDGEMENT

Support for this work was given by 2002 and 2004 Dreyfus Senior mentor awards and NSF/DMR grant 9612873 at SJSU, and DOE at SSRL and LBNL-ALS. We are very grateful to Prof. Gina Corongiu and E.

Clementi, who developed the MOLECOLE and the original METTECC codes [12] that allow large SCF and in particular, molecular orbital calculations for a nano particle. Professor Yao W. Liang, Cavendish Laboratory, Cambridge University is thanked for discussion and for moral support. We thank Drs. A. Mehta and P. Nachimuthu who gave us very valuable help in the data acquisition at SSRL and LBNL-ALS respectively.

REFERENCES

1. J.V. Acrivos and O. Stradella, *International Journal of Quantum Chemistry*, **46**, 55(1993)
2. M. A. Navacerrada and J.V. Acrivos, *NanoTech 2003*, **1**, 751 (2003) and ref. therein.
3. Z.-X. Shen, W.E. Spicer, D.M. King, D.S. Dessau, B.O.Wells, *Science* **267**, 343 (1995)
4. M. A. Navacerrada, M. L. Lucía and F. Sánchez-Quesada, *Europhys. Lett* **54**, 387, 2001 and references therein.
5. A. Bianconi et al, *Phys. Rev.* **B38**, 7196 (1988)
6. M. Hentschel, D. Ullmo and H. Baranger, *Phys. Rev. Lett.* **93**, 176807 (2004)
7. J.V. Acrivos et al. to be published
8. G. Koster, T.H. Geballe and B.Moyzhes, *Phys. Rev.* **B66**, 085109 (2004)
9. J.V. Acrivos, *Microchemical Journal* (2005) in press
10. L.I. Sciff, "Quantum Mechanics", McGraw Hill Book Co. Inc, 1949
11. S. Murakami, N. Nagaosa and S. C. Zhang, *Science* **301**, 1348 (2003)
12. E. Clementi, ed., "Methods and Techniques in Computational Chemistry", "METTECC-94 A, B and C", STEF, Cagliari (1993)